Experimental investigation of adaptive beam with embedded devices

Abdulmalik A. Alghamdi and Abhijit Dasgupta

Mechanical Engineering Department
University of Maryland at College Park

ABSTRACT

In this paper we are presenting the experimental dynamic response of an adaptive beam containing embedded mini-devices (sensors and actuators). The specimen used is a cantilever beam made of ALPLEX plastic as host material and PZT-5H as active devices for sensing and actuation. The experimental setup, and experimental results are presented and discussed. The capability of mini-actuators to change the dynamical behavior of the adaptive beam is demonstrated through adaptive stiffening and adaptive damping examples.

Keywords: adaptive structures, eigenstrain techniques, mini actuators, adaptive stiffening, adaptive damping.

2. INTRODUCTION

Adaptive materials and intelligent systems have been the focus of researchers for quite sometime. Adaptive structures have been used in the area of active vibration control by many researchers, see for example [Hagood et al, 1990], [Tzou and Tseng, 1990], [Crawley and Lazarus, 1991], and [Ha et al, 1992].

Most present-day adaptive structural systems consist of relatively large surface-mounted "active" elements such as actuators and sensors. These elements cause reliability problems due to high stress concentrations, poor interfacial bonding, change in the boundary conditions, etc. These limitations can be overcome by having distributions of embedded mini-active elements. However, embedding produces three-dimensional stress interactions which are more difficult to model than those arising in surface-mounted devices.

Eshelby's technique offers a convenient method to model the mechanical interactions in systems with embedded mini-devices. Eshelby's equivalent inclusion method has been previously used by the authors to model the elastic interaction between actuators/sensors and the host, by using appropriate Green's functions. The authors have presented numerous papers in developing analytical solutions for embedded mini-devices using eigenstrain techniques, see for example [Dasgupta and Alghamdi, 1992], [Alghamdi and Dasgupta, 1993a], [Alghamdi and Dasgupta, 1993b], and [Dasgupta and Alghamdi, 1994].

This paper experimentally investigates the dynamic response of a "smart" beam having embedded mini-devices. Results of the experimental behavior of a vibrating beam with embedded

0-8194-1775-0/95/$6.00

arrays of mini-devices are presented. Sensors are used to measure the external loads and their outputs are used in a closed-loop feedback circuit to excite the actuators.

The experimental study of the adaptive structure presented in this paper is different from most of the published articles, see [Baily and Hubbard, 1985], [Crawley and de Luis, 1987], [Hagood and Flotow, 1991], [Hollkamp, 1993]. The difference is because the size of the sensors and actuators which is relatively small in comparison to devices used by other researchers. It is believed that reliability improves and obtrusivity decreases as the size of the embedded devices decreases, for the same actuation authority and device volume fraction.

Experimental study of the dynamical behavior of an adaptive beam with mini-devices is the focus of this paper. Adaptivity of the beam is illustrated through adaptive stiffening and adaptive damping of the cantilever beam.

As the beam in Figure (1) vibrates, sensors in the upper row are deformed and due to piezoelectricity effect, they produce electrical fields. If the electrical field is amplified with a constant gain and sent to the actuator in the lower row (position feedback), this will result in adaptive stiffening [Alghamdi and Dasgupta, 1993c]. If the electrical field is made proportional to the rate of the electrical voltage produced by the sensors (velocity feedback), then this will result in adaptive damping [Dasgupta and Alghamdi, 1994].

3. ADAPTIVE CANTILEVER BEAM

Figure (1) shows the specimen used in the test. This beam was fabricated in Photomechanics Laboratory at the University of Maryland, College Park. Material properties are given in Figure (1). The host material, ALPLEX, is a polymer initially in liquid state. It consists of a polymer resin and a hardener to solidify. The specimen is made by a molding process by using two aluminum plates as the mold. The cross-sectional shape of the beam is machined into the mold plates. Sides grooves are made to hold the PZT elements. The beam is fabricated at room temperature by injecting the ALPLEX inside the mold. The mold is removed forty eight hours after casting. Post curing is done for 3 days at room temperature for the beam to harden before it is tested. After solidification ALPLEX is transparent and any void or gas bubble is easily detected visually. The beam width is 1" and the drawing in Figure (1) is not to scale.

Two rows of piezoceramic (PZT) devices are embedded within the ALPLEX beam symmetrically about the beam midplane as shown in Figure (1). Each device has a volume of 0.22% of the beam volume. The PZT elements are oriented so that the polarization direction is perpendicular to the beam length-width plane. PZT elements have the same width as the beam.

4. EXPERIMENTAL SETUP

Figure (2) illustrates the experimental setup. The upper row devices are used as sensors while the lower row devices are used as actuators. The first two pairs (pair denotes a sensor and the

corresponding actuator on the opposite side) from the fixed end are used to control the vibration of the beam. The third pair is used to excite the beam for forced vibration response analysis. Devices of the third pair are excited 180° out-of-phase to excite a pure bending mode. For free vibration, the excitation voltage of the third pair is set to be zero. The sensor in the last pair is connected to the Dynamic Analyzer, while the remaining device in the fourth pair is used as a sensor to record the vibration history in time domain.

Sensor readings from Pairs I and II are amplified using charge amplifiers. The output is then passed through a phase shifter to adjust the phase between the electrical field generated by the sensor in the upper row and the electrical field sent to actuator in the lower row. A frequency filter is utilized to cut off higher frequency signals which tend to create noise in the system. A differentiator is used only for velocity feedback. In the case of position feedback, the differentiator is removed from the system. A power amplifier is used to amplify the signal before it goes to the actuators. A digital oscilloscope was used to capture the beam response in time domain. Data stored in the oscilloscope was downloaded to a computer for analysis.

5. RESULTS AND DISCUSSIONS

5.1 Adaptive stiffening

Figure (3) represents the dynamic response of the beam due to a finger pulse at the free end. The figure shows the time response for the system at three different conditions. The time response shown represents normalized sensor voltage. The solid line is the time response with all devices passive (zero applied electrical field, E = 0 V/mm). The dashed line represents the response with one device active (pair I) at E = 320 V/mm. The dotted line is for two devices active with actuator I at E = 320 Volts. The field in actuator II is smaller than the field in actuator I since the output of sensor II is smaller than the output of sensor I. It can be seen that as the number of active devices increases, the time period of the structure response decreases. In other words, the first fundamental frequency increases. The change in the period is very small and can be seen in Figures (4) and (5) clearly. Stiffening is accompanied by some damping since the induced strains at actuators are opposing the natural vibration. Damping due to position feedback was reported in the literature (see for example [Fanson et al, 1989]). It is worth mentioning at this point that the small change in the dynamic response is due to the small volume fraction of the devices which is only 0.4% for each pair (0.2% for sensor and 0.2% for actuator).

Figures (4) and (5) represent the frequency response function (FRF) of the adaptive beam for sinusoidal sweep excitation. The excitation frequency is swept from 20 to 30 Hz because the first natural frequency is approximately 24 Hz. Figure (4) shows the magnitude of the FRF on a linear scale, while Figure (5) shows the phase shift of the FRF on a linear scale. These two figures indicate very clearly, the stiffening in the system as the number of active device pairs increase. The solid line represents the system performance at zero electrical field and no active pair. The dashed and dashed-dotted lines represent the system with actuator I at E = 240 V/mm and one and two active device pairs, respectively. The decrease in the amplitude of the FRF is due to the damping accompanying the stiffening effect.

The effect of changing electrical field, by changing the gain factor of the power amplifier, is shown in Figure (6). The y-axis is the fundamental frequency of the adaptive beam normalized with respect to the frequency of the passive beam (zero excitation voltage). These values of the fundamental frequency are the corresponding frequencies of the peaks of FRF plots obtained by the Dynamic Analyzer. The x-axis is the electrical field applied to actuator I. The figure shows the system behavior for one (n=1) and two (n=2) active pairs of devices. It can be seen that as the electrical field increases, the induced strain increases, and hence the stiffening increases.

5.2 Adaptive damping

In this setup, the feedback is made proportional to the rate of the sensor output, by differentiation of the sensor output signal before feeding it to the actuator. Figure (7) shows the time response of the adaptive beam due to a finger pulse at the free end. The response is normalized by the measured initial displacement. The solid line represents the response of the passive (zero electrical field). In this case, beam is allowed to damp due its structural damping only. The dashed and dotted lines represent the system output for actuator I at E = 60 V/mm, and n = 1 and 2, respectively. The beam damps faster as the number of active pairs increases, and this is accompanied by some softening represented by the increase in time period.

Forced vibration control is shown in Figures (8) and (9) for sweep sine excitation. Again magnitude and phase of the FRF are displayed. Solid lines in both figures represent FRF at zero active device and zero excitation voltage, while the dashed and dashed-dotted lines represent the FRF for n = 1 and 2, respectively with actuator I at E = 240 V/mm. As we can see, damping improves as the number of active pair increases. The change in damping due to activation of the second pair is less than that of the first pair because of the less authority that the second pair has. Damping is expected to improve as the device volume fraction increases.

6. CONCLUSIONS

An adaptive beam was manufactured and tested for active vibration control by means of adaptive stiffening and damping experiments. Adaptive stiffening of the adaptive beam was achieved experimentally by using position feedback control, while adaptive damping was achieved by using velocity feedback control. This paper experimentally demonstrates the capability of mini-actuators to control the dynamic characteristics of a passive beam. The experimental setup used is very simple one and it does not need any complex control scheme. In future papers we will compare these results with analytical prediction obtained by eigenstrain analysis.

7. ACKNOWLEDGEMENT

The author would like to thank King Abdulaziz University, Jeddah, Saudi Arabia for supporting this research. Also, this research is partially supported by Army Research Office of the United States Army. The project monitor is Dr. Gary Anderson. We thank Mr. P. Chen of the Aerospace Engineering Department at University of Maryland College Park for presenting this paper at the conference.

8. REFERENCES

Alghamdi, A., and Dasgupta, A., "Interaction Mechanics Between Embedded Micro-Actuators and the Surrounding Host in Adaptive Structures," *Proceedings of SPIE's 1993 North American Conference on Smart Structures and Materials*, edited by N. W. Hagood and G. J. Knowles, Albuquerque, New Mexico, pp. 317-328, 1993a.

Alghamdi, A., and Dasgupta, A., "Micromechanical Dynamic Analysis of an Adaptive Beam with Embedded Distributions of Piezoelectric Actuator/sensor Devices," *Adaptive Structures and Material Systems, The 1993 ASME Winter Annual Meeting*, AD-Vol. 35, edited by G. P. Carman and E. Garcia, New Orleans, Louisiana, pp. 121-128, 1993b.

Alghamdi, A., and Dasgupta, A.,"Frequency Prediction of a "Smart" Beam Using Eshelby Techniques with Linear distributed Strains," *Proceedings of American Society for Composites, Eight Technical Conference*, Cleveland, Ohio, pp. 174-183, 1993c.

Bailey, T. and Hubbard, J. E. Jr., "Distributed piezoelectric-polymer active vibration control of a cantilever beam," *AIAA Journal of Guidance, Control and Dynamics*, Vol. 8, No. 5, pp. 605-611, Sep-Oct, 1985.

Burke, S. E. and Hubbard, J. E. Jr., "Active Vibration Control of a Simply Supported Beam Using a Spatially Distributed Actuator," *IEEE Control Systems Magazine*, Vol. 7, No. 6, pp. 25-30, August 1987.

Crawley, E. F., and de Luis, J., "Use of piezoelectric actuators as elements of intelligent structures," *AIAA Journal*, Vol. 25, No. 10, pp. 1373-1385, 1987.

Crawley, E. F., and Lazarus, K. B., "Induced strain actuation of isotropic and anisotropic plates," *AIAA Journal*, Vol. 29, No. 6, pp. 944-951, June 1991.

Dasgupta, A., and Alghamdi, A., "Interaction mechanics between embedded micro-actuators and the surrounding host in smart structures," *Proceedings of the American Society for Composites, Seventh Technical Conference*, University Park, Pennsylvania, pp. 919-928, 1992.

Dasgupta, A., and Alghamdi, A. A., "Transient response of an adaptive beam with embedded piezoelectric microactuators," *Proceedings of SPIE's 1994 North American Conference on Smart Structures and Materials*, edited N. W. Hagood, Orlando, Florida, pp. 153-164, 1994.

Fanson, J. L., Blackwood, G. H., and Chu, C-C., "Active-member control of precision structures", *AIAA Paper* 89-1329.

Ha, S. K., Keilers, C. and Chang, F-K., "Finite element analysis of composite structures containing distributed piezoceramics sensors and actuators," *AIAA Journal*, Vol. 30, No. 3, pp. 772-780, March 1992.

Hagood, N. W., Chung, W. H., and Flotow, A. V., "Modeling of piezoelectric actuator dynamics for active structural control," *Journal of Intelligent Material Systems and Structures*, Vol. 1, No. 3, pp. 327-354, July 1990.

Hagood, N. W., and Flotow, A. Von, "Damping of structural vibrations with piezoelectric materials and passive electric networks," *Journal of Sound and Vibration*, Vol. 146, No. 2, pp. 243-268, 1991.

Hollkamp, J. J., "Multimodal passive vibration suppression with piezoelectrics", *AIAA Paper* 93-1683.

Tzou, H. S. and Tseng, C. I., "Distributed piezoelectric sensor/actuator design for dynamic measurement/control of distributed parameter systems: A Piezoelectric finite element approach," *Journal of Sound and Vibration*, Vol. 138, No. 1, pp. 17-34, 1990.

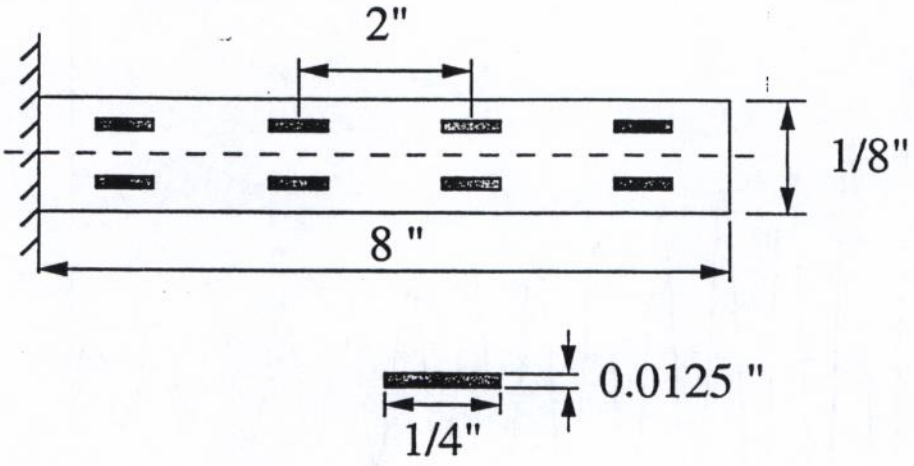

HOST : ALPLEX
E = 2.3 GPa
υ = 0.3

DEVICES : PZT-5H
E = 64 GPa
υ = 0.31
d_{31} = 274 e-12 m/V

Figure (1): Schematic Drawing of the Adaptive Beam.

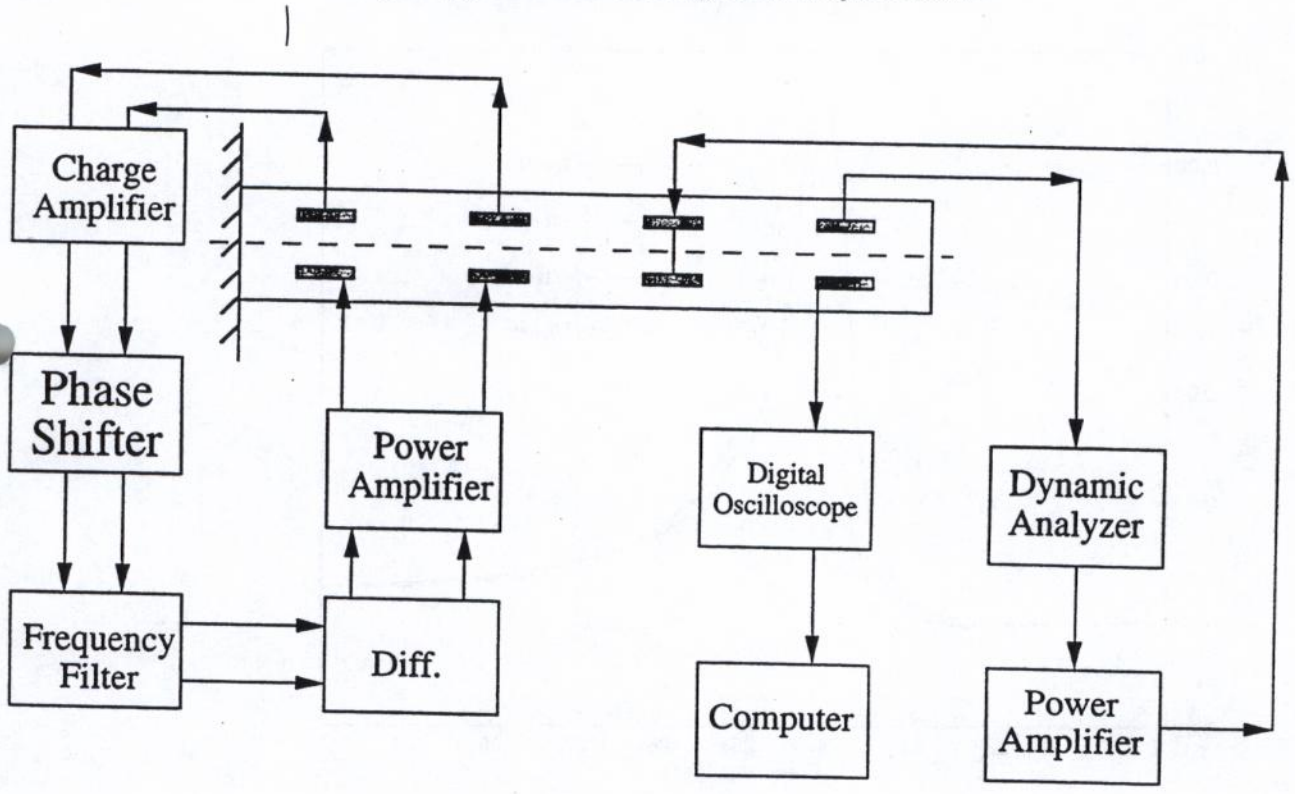

Figure (2): The Experimental Setup.

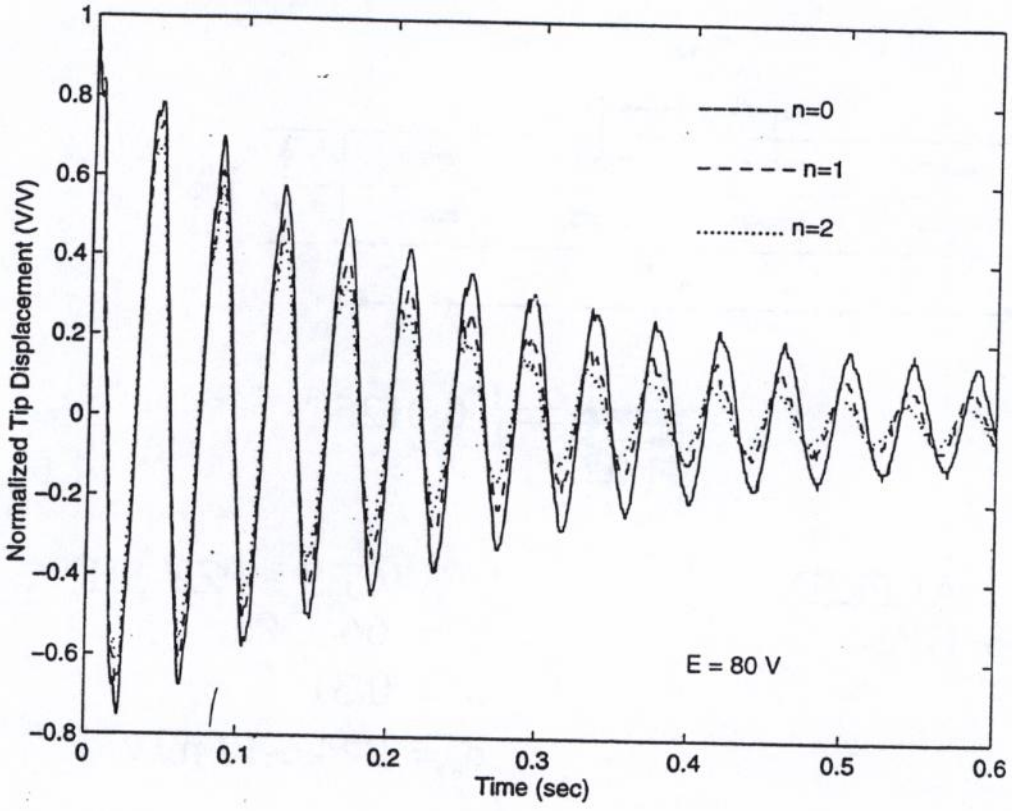

Figure (3): Adaptive Stiffening in Time Domain.

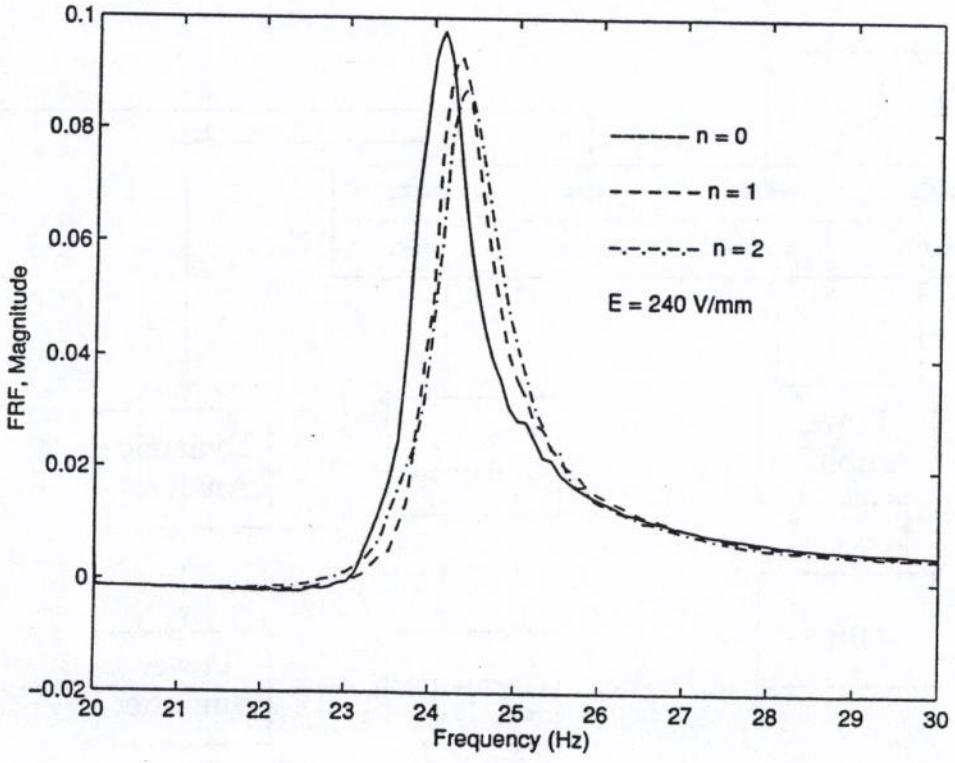

Figure (4): Adaptive Stiffening in Frequency Domain (Magnitude).

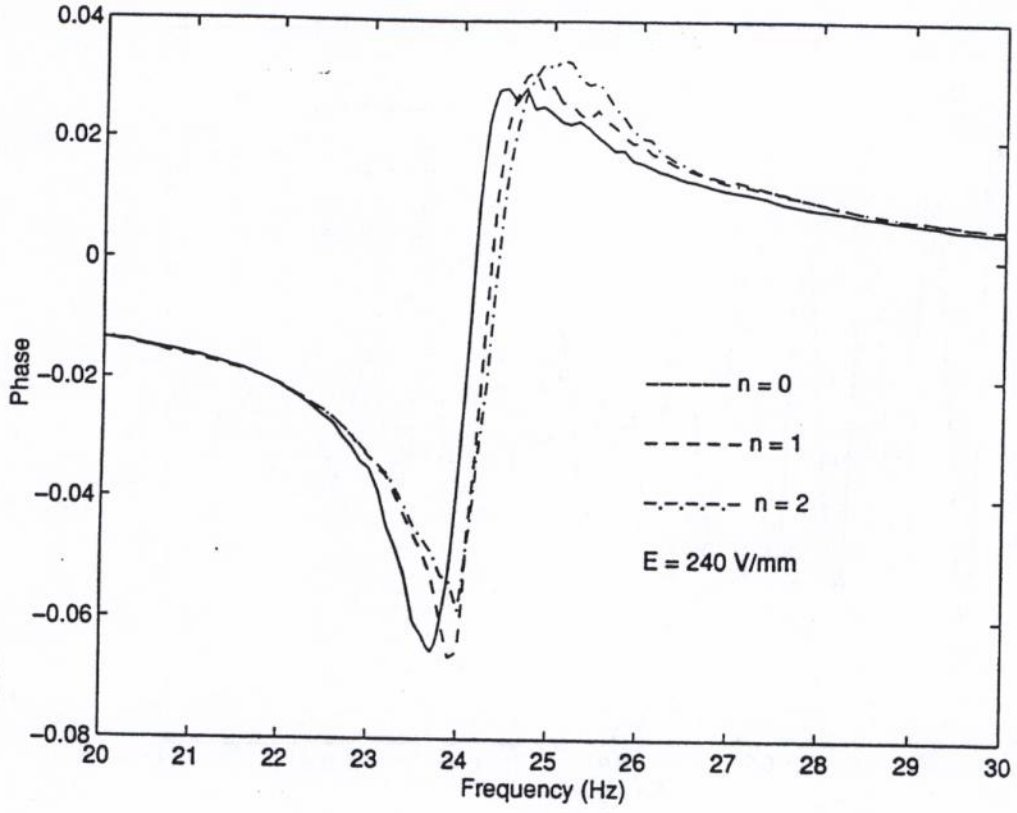

Figure (5): Adaptive Stiffening in Frequency Domain (Phase).

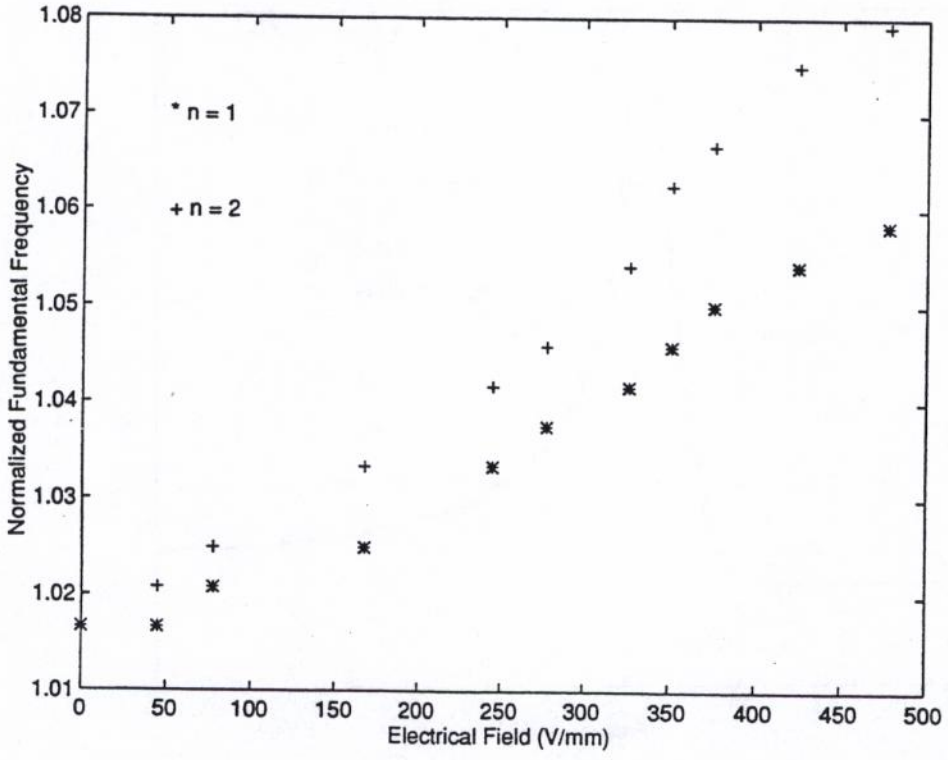

Figure (6): Effect of Electrical Field on Stiffening.

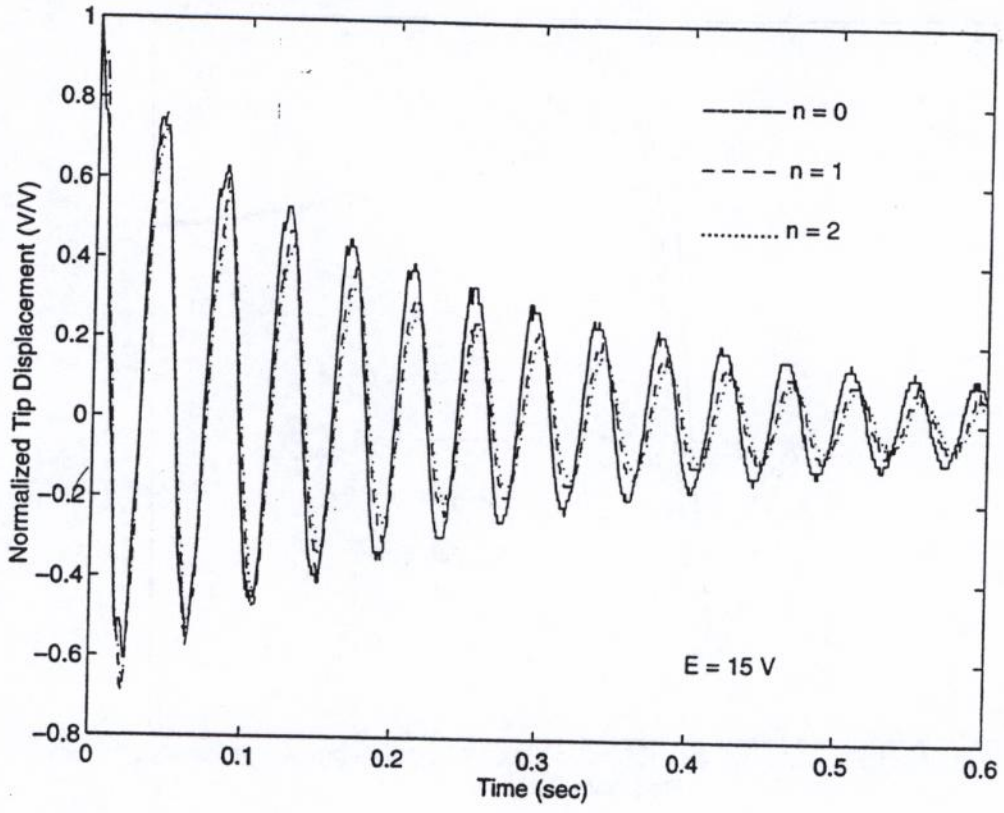

Figure (7): Adaptive Damping in Time Domain.

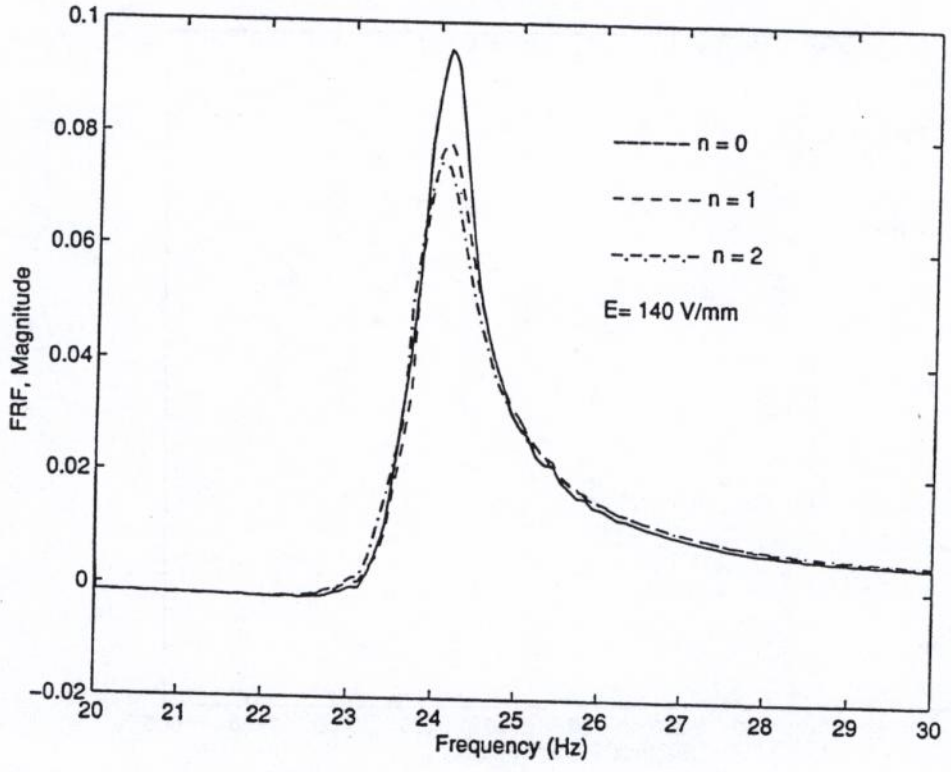

Figure (8): Adaptive Damping in Frequency Domain (Magnitude).

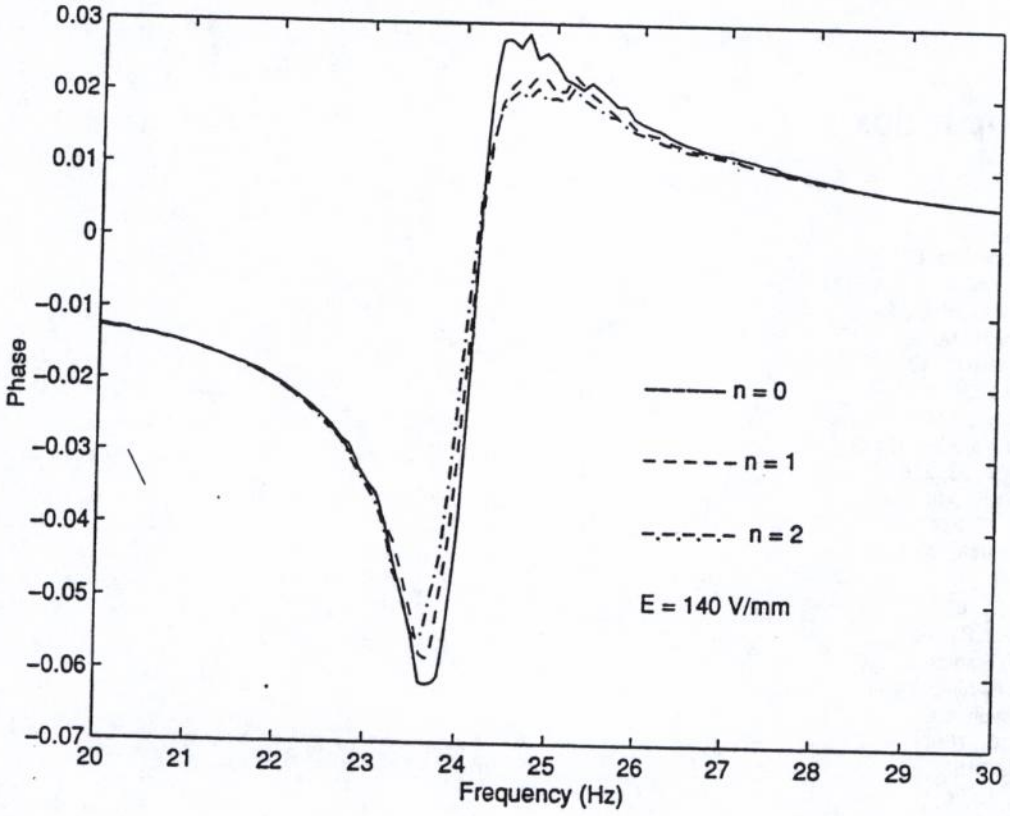

Figure (9): Adaptive Damping in Frequency Domain (Phase).

Author Index